# Safety Verification of Seismic Isolation System Using Rubber Bearing Against Long-Period Earthquake Motion.


**M. Hikita, E. Takaoka & A. Kondo**
*Kajima Corporation, Tokyo, Japan*

**T. Nishimura & S. Yamamoto**
*Shimizu Corporation, Tokyo, Japan*

**M. Takayama**
*Fukuoka University, Fukuoka, Japan*

**M. Kikuchi**
*Hokkaido University, Hokkaido, Japan*

**M. Iiba**
*Building Research Institute, Ibaraki, Japan*

**SUMMARY**
In recent years, long-period earthquake motion has become a source of nationwide public concern and interest in Japan. Long-period earthquakes cause significant swaying motion lasting several minutes in super-high-rise buildings and seismically isolated structures. Although laminated rubber bearings are widely used for the latter, much remains unknown about their characteristics in response to repetitive motion and their ultimate performance. To clarify the ultimate state of these bearings, the authors carried out multi-cyclic loading tests using scaled specimens of lead rubber bearings and high damping rubber bearings, which are regarded as typical laminated rubber bearing types. The results showed that temperature rise of specimen led to reduced yield strength and damping performance. Even with identical levels of cumulative deformation, the yield strength fell as the amplitude increased

*Keywords: Long-period earthquake motion, Laminated rubber bearing, Seismic isolation, Multi-cyclic loading*

## 1. OVERVIEW

Large earthquakes in recent years have caused long-period ground motion around Japan, and the resulting impacts on super-high-rise buildings and seismically isolated buildings have prompted nationwide public concern. The 2011 earthquake off the Pacific coast of Tohoku triggered long-period ground motion on the Kanto Plain. Earthquakes are expected to occur in the regions of Tokai, Tonankai, Nankai and adjacent areas in the near future, and the Kanto, Nobi and Osaka plains (where major Japanese cities such as Tokyo, Nagoya and Osaka are located) are likely to be exposed to long-period ground motion with even greater amplitudes.
Long-period ground motion continues for longer than that generated by the seismic waves previously considered in seismic response analysis. Accordingly, it is necessary to evaluate the methods used for assessing the performance of seismically isolating devices against long-period ground motion and their influence on building response, and to reconsider the related mechanical characteristics.
Although laminated rubber bearings are widely used for seismically isolated buildings, much unknown things remains about their characteristics in response to repetitive motion and their ultimate performance. In verifying the safety of such bearings against long-period ground motion, it is important to clarify performance in response to large cumulative deformation and high amounts of cumulative energy absorption resulting from repetitive swaying motion. From this background, the authors carried out multi-cyclic loading tests using scaled specimens of lead rubber bearings (LRBs) and high damping rubber bearings (HDRBs), which are regarded as typical laminated rubber bearing.
Previous studies on LRB have reported that the temperature of their lead plugs rises and their yield strength falls in response to prolonged repetitive swaying motion[1)]. For HDRB too, it is known that the

temperature rises and the horizontal performance (equivalent horizontal stiffness, equivalent viscous damping, amount of energy absorbed) not only deteriorates as a result of such motion but also depends on motion frequency, loading history and temperature[2]. The experiment in this study was designed in consideration of these characteristics, and is described in the following chapter.

## 2. EXPERIMENTAL METHODS

The specimen prototype was a laminated rubber bearing with a diameter of 1,000 mm. In order to avoid changing the thermal capacity per unit volume, the thicknesses of the rubber layer and the steel plate were reduced as much as possible on the same scale.
The LRB specimens were 1/2-scale models of the prototype, and LRB with a shear modulus of 0.392 N/mm$^2$ were used. Two types of specimens were adopted. One was a laminated rubber bearing containing one lead plug (referred to here as the single-lead-plug type), which is generally used for buildings. The diameter of the lead plug was 1/5 that of the rubber in the bearing. The other specimen was a laminated rubber bearing containing three lead plugs (referred to here as the triple-lead-plug type). The total sectional area of the three plugs was equivalent to that of the single-lead-plug type. An outline of the specimens is given in Figure 1, which shows single-lead-plug types (#1L, #2L and #3L) and triple-lead-plug type (#4L). Table 1 shows the dimensions of the LRB for the prototype and the specimens.
The HDRB specimens were 1/4-scale models of the prototype, and HDRB with a shear modulus of 0.620 N/mm$^2$ (for a shear strain of $\gamma$ = 100%) were adopted. Figure 2 gives an outline of the four specimens adopted, and Table 2 details the dimensions of the HDRB used for the prototype and specimens.

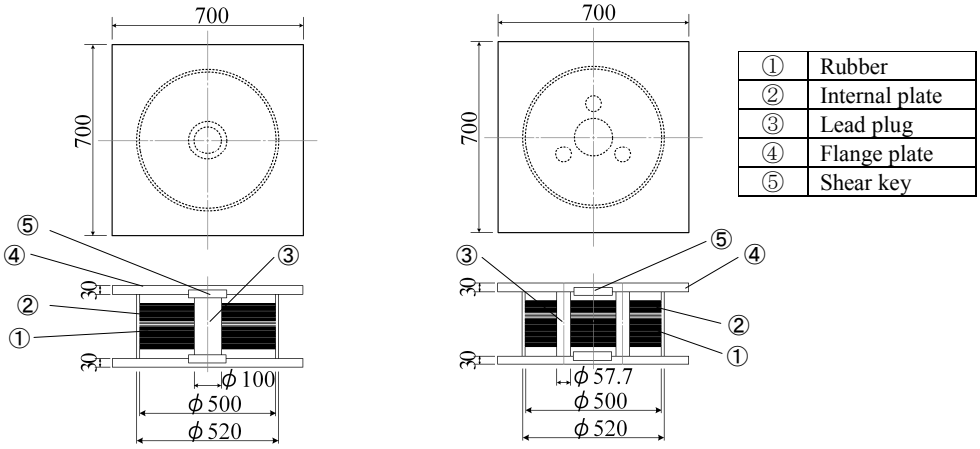


(a) Single-lead-plug type (#1L, #2L and #3L)

(b) Triple-lead-plug type (#4L)

**Figure 1.** Outline of specimens (LRB)

**Table 1.** Dimensions of lead rubber bearings (LRB)

| | Prototype | Models (1/2 scale) | |
|---|---|---|---|
| | | Single-lead-plug type (#1L,#2L,#3L) | Triple-lead-plug type (#4L) |
| Number of specimens | - | 3 | 1 |
| Diameter of rubber $D_L$ (mm) | 1,000 | 500 | 500 |
| Number of lead plugs | 1 | 1 | 3 |
| Diameter of plugs (mm) | 200 | 100 | 57.7 |
| Number of rubber sheets | 33 | 33 | 33 |
| Rubber sheet thickness $t_L$ (mm) | 6.0 | 3.0 | 3.0 |
| Total rubber thickness $h_L$ (mm) | 198 | 99 | 99 |
| Internal plate thickness (mm) | 4.4 | 2.2 | 2.2 |
| Shape factor ($D_L/4t_L$) $S_1$ | 41.7 | 41.7 | 41.7 |
| Second shape factor ($D_L/h_L$) $S_2$ | 5.1 | 5.1 | 5.1 |

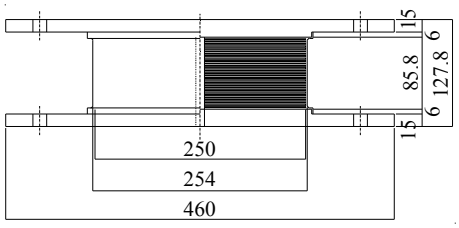


(#1H, #2H, #3H and #4H)

**Figure 2.** Outline of specimens (HDRB)

**Table 2.** Dimension of high damping rubber bearings (HDRB)

| | Prototype | Model (1/4 scale) |
|---|---|---|
| Number of specimens | - | 4 |
| Diameter of rubber $D_H$ (mm) | 1,000 | 250 |
| Number of rubber sheets | 30 | 30 |
| Rubber sheet thickness $t_H$ (mm) | 6.7 | 1.7 |
| Total rubber thickness $h_H$ (mm) | 201 | 51 |
| Internal plate thickness (mm) | 4.4 | 1.2 |
| Shape factor ($D_H/4t_H$) $S_1$ | 36.4 | 35.3 |
| Second shape factor ($D_H/h_H$) $S_2$ | 4.98 | 4.9 |

In the tests, sinusoidal waves and earthquake response waves representing long-period ground motion were applied in the horizontal direction at a constant axial stress of 15 N/mm$^2$ with scaled-down models. The parameters of the sine waves were shear strain γ (= horizontal deformation / total rubber thickness) and the number of repetitions. The period of sine wave was 4 seconds. The results of previous research on seismically isolated building behavior in response to long-period ground motion indicated cumulative deformation of approximately 20 to 30 m and maximum displacement of around 500 to 600 mm in seismically isolated devices[3]. Based on these outcomes, the shear strain amplitude of the sine wave in this study was set up to three levels (200%, 100% and 50%), and the number of repetitions was set to produce cumulative deformation of 25 m, 50 m and 100 m in line with the expected effects of long-period ground motion.

The displacement time history of the earthquake response was determined from related analysis of a seismically isolated building supported by rubber bearings. The input wave of the analysis was the earthquake expected to occur in the regions of Tokai and Tonankai in the near future. Two earthquake response waves (referred to hear as EQ-T-TN and EQ-T-TN×1.5) were adopted[4], and the maximum shear strain of the waves are 136% and 287%, respectively. Figure 3 shows the time history of the earthquake response wave EQ-T-TN.

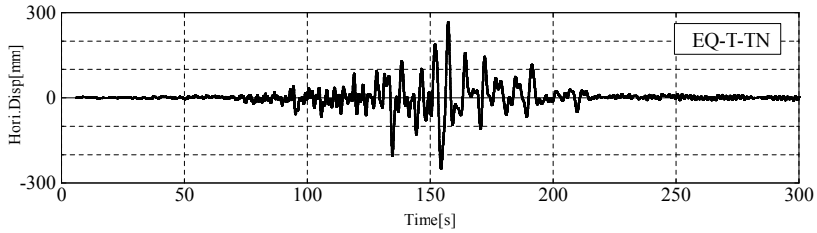


(Time history multiplied by the reduction rates to create the experiment displacement time history.)

**Figure 3.** Time history of earthquake response

Table 3 lists the loading cases of LRB, and Table 4 shows those of each LRB specimen. The shear strain amplitude of the sine wave (from L1 to L6) was divided into three levels (200%, 100% and 50%). In L1, L2 and L3, the number of repetitions was set to produce cumulative deformation of approximately 25 m, meaning that the cumulative deformation of the prototype laminated rubber bearing was 50 m. Cases L1, L2 and L3 involved testing with long-period ground motion. In order to

clarify the ultimate characteristics, cumulative deformation was doubled in the tests for L4, L5 and L6. Although the time separating experiments was taken as 30 minutes in principle, when the specimen temperature was higher than 25°C, the interval was simply continued until the temperature fell to 25°C.

**Table 3.** Loading cases (LRB)

| No. | Input wave | Case | Period T(sec) | Shear strain γ(%) | Maximum velocity (cm/s) | Number of repetitions (cycle) | Cumulative deformation (m) |
|---|---|---|---|---|---|---|---|
| L1 | Sine | Long-period ground motion*1 | 4 | 50 | 8.0 | 125 | 24.75 |
| L2 | Sine | | 4 | 100 | 15.9 | 60 | 23.76 |
| L3 | Sine | | 4 | 200 | 31.9 | 30 | 23.76 |
| L4 | Sine | Ultimate characteristic*2 | 4 | 50 | 8.0 | 250 | 49.50 |
| L5 | Sine | | 4 | 100 | 15.9 | 120 | 47.52 |
| L6 | Sine | | 4 | 200 | 31.9 | 60 | 47.52 |
| L7 | EQ-T-TN | - | - | 136 | - | - | 13.00 |
| L8 | EQ-T-TN×1.5 | - | - | 287 | - | - | 17.20 |

*1: Cumulative deformation assuming long-period ground motion.
*2: Cumulative deformation for clarification of the ultimate characteristic.

**Table 4.** Loading cases for each specimen (LRB)

| Specimen No. | Type of specimen | Case | |
|---|---|---|---|
| #1L | Single-lead-plug type | L1 | γ = 50%, 125 cycles |
| | | L2 | γ = 50%, 250 cycles |
| | | L7 | Earthquake response $\gamma_{max}$ = 136% |
| #2L | | L3 | γ = 100%, 60cycles |
| | | L4 | γ = 100%, 120cycles |
| | | L8 | Earthquake response $\gamma_{max}$ = 287% |
| #3L | | L5 | γ = 200%, 30cycles |
| | | L6 | γ = 200%, 60cycles |
| #4L | Triple-lead-plug type | L2 | γ = 200%, 250cycles |
| | | L6 | γ = 200%, 60cycles |
| | | L8 | Earthquake response $\gamma_{max}$ = 287% |

Table 5 lists the loading cases of HDRB. Multi-cycle sine wave load testing of HDRB has been reported in a number of previous studies[ex.1)]. Among these, cumulative deformation of more than 70 m was seen. Accordingly, the number of repetitions in HDRB experiments was set to produce cumulative deformation of around 100 m.
In H1, H2 and H3, the parameters were shear strain and number of repetitions. As described above, HDRB performance is known to depend on the characteristics of temperature and loading hysteresis. The initial specimen temperature and loading history were therefore added as experimental parameters. Temperature dependence was confirmed by comparing the specimen with the initial temperature at 30°C to that at 0°C (H4 and H5). Additionally, to verify loading hysteresis dependence, loading with patterns of gradual-increase and gradual-decrease was conducted (H6 and H7). In gradual-increase loading (H6), shear strain was gradually raised in a pattern of 50%, 100%, 200% and 250%. Conversely, shear strain was gradually reduced in a pattern of 250%, 200%, 100% and 50% in gradual-decrease loading (H7). The cumulative deformation observed in both tests was about 100 m. The earthquake response wave was the EQ-T-TN form shown in Figure 3. In the experiment, the characteristics of the EQ-T-TN were determined during the period of 60 – 210 seconds (the main part of the wave), and four connections were made. In this case, the cumulative deformation was assumed to be 50 m in the prototype.

**Table 5.** Loading cases for each specimen (HDRB)

| Specimen No. | Case No. | Case | Input wave | Period T (sec) | Shear strain γ (%) | Number of repetitions (cycles) | Cumulative deformation (m) | Initial temp. (°C) |
|---|---|---|---|---|---|---|---|---|
| #1H | H1 | Ultimate characteristic | Sine | 4 | 50 | 1,000 | 104 | 20 |
| | H2 | | Sine | 4 | 100 | 500 | 102 | 20 |
| | H3 | | Sine | 4 | 200 | 250 | 102 | 20 |
| #2H | H4 | Initial temp. of specimen | Sine | 4 | 200 | 250 | 102 | 0 |
| | H5 | | Sine | 4 | 200 | 250 | 102 | 30 |
| #3H | H6 | Loading history (gradual-increase) | Sine | 4 | 50 | 245 | 25.0 | 20 |
| | | | Sine | 4 | 100 | 122 | 24.9 | |
| | | | Sine | 4 | 200 | 61 | 24.9 | |
| | | | Sine | 4 | 250 | 49 | 25.1 | |
| #4H | H7 | Loading history (gradual-decrease) | Sine | 4 | 250 | 49 | 25.1 | 20 |
| | | | Sine | 4 | 200 | 61 | 24.9 | |
| | | | Sine | 4 | 100 | 122 | 24.9 | |
| | | | Sine | 4 | 50 | 245 | 25.0 | |
| | H8 | Ultimate characteristic | EQ-T-TN*3 | - | 136 | - | - | 20 |

*3 Applied four times in a row.

During the experiment, a 10-mm-thick heat-insulating board was used to separate the specimen and the loading equipment.
The items measured were the axial force, horizontal force, horizontal displacement and temperatures of the specimen. The temperatures of the rubber bearings were monitored continuously using thermocouples in the specimens both during and after the experiment. Figure 4 and Figure 5 shows examples of the temperature measurement points.

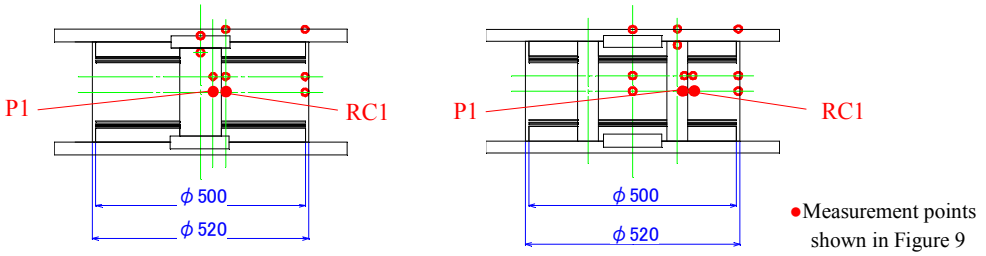


(a) Single-lead-plug type (b) Triple-lead-plug type

**Figure 4.** Temperature measurement points (LRB)

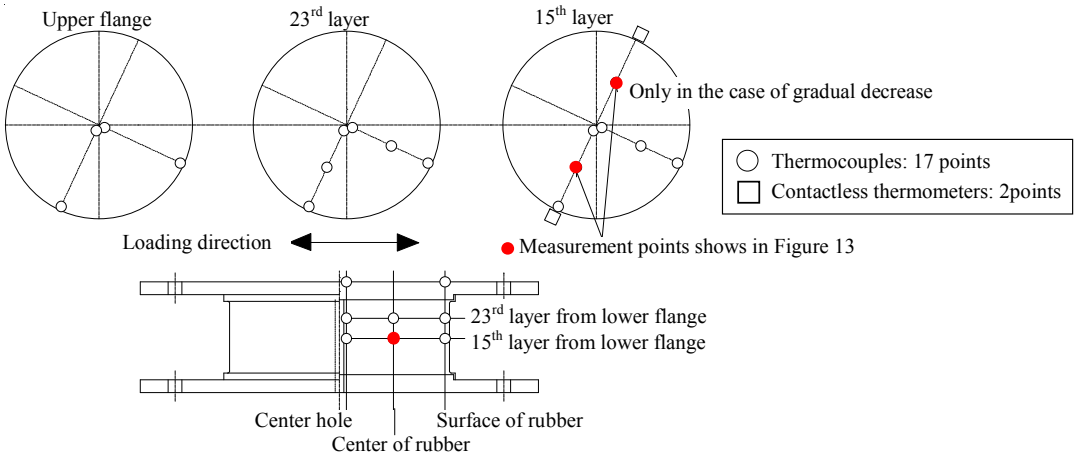


**Figure 5.** Temperature measurement points (HDRB)

## 3. RESULTS

### 3.1 Lead Rubber Bearing Experiments

*3.1.1. Method of determining LRB hysteresis characteristics*

Changes in characteristics were determined based on the yielding load $Q_d$ and the stiffness $K_d$ after yielding. Based on Figure 6, $Q_d$ and $K_d$ are represented by Eqn. 3.1 and 3.2. The properties of the rubber bearings were determined by standardizing the $Q_d$ and $K_d$ values for each cycle. $Q_{du}$ and $Q_{dd}$ represent the positive and negative yielding loads at displacement = 0, respectively, $K_{du}$ and $K_{dd}$ are the inclinations of the lines connecting points that have values of ± 50% for each maximum displacement, and ΔW (that is, the energy absorbed in one cycle) represents the areas enclosed by the curves.

$$Q_d = \frac{|Q_{du}| + |Q_{dd}|}{2} \quad (3.1)$$

$$K_d = \frac{|K_{du}| + |K_{dd}|}{2} \quad (3.2)$$

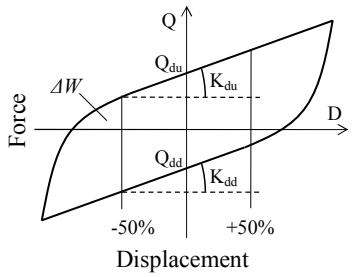


**Figure 6.** Definitions of $Q_d$, $K_d$ and ΔW

*3.1.2. Experiment results*

Figure 7 shows the relationships between horizontal force Q and horizontal displacement D for loading cases L4, L5 and L6. It can be seen that the shapes of the hysteresis curves are stable, but the area they enclose decreases as the number of repetitions increases. In the cases with half the number of repetitions (L1, L2 and L3), the Q-D relationships are almost the same (not shown here). The hysteresis curves after the experiments also show close mutual correspondence. Specifically, the curves became stable with the number of repetitions seen in long-period ground motion (as L1, L2 and L3), and the hysteresis characteristics did not change significantly with numbers of repetitions exceeding this level. Comparison of Figures 7 (c) and (d) suggests that the shapes of hysteresis curves for the single-lead-plug type and the triple-lead-plug type with 200% shear strain exhibit mutual similarity. However, the area enclosed by the curve of the triple-lead-plug type is a little larger than that of single-plug type.

Figure 8 shows changes in $Q_d$ and $K_d$ normalized with the third-cycle value. It can be seen from Figure 8 (a) that the $Q_d$ values began to drop after the start of loading. The decline of $Q_d$ in the same cycle was remarkable when the shear strain amplitude was larger. Although the $Q_d$ values fell rapidly up to about 50 cycles, minimal decrease was seen after 50 cycles. $Q_d$ fell in proportion to γ increased, and by the end of the study was about 0.5 in L6 (γ = 200%, 60 cycles).

The change in $K_d$ was small when the shear strain γ was 100% and 200%, but was large when γ was 50%. This is thought to be due to the influence of lead plug stiffness with a γ value of 50%.

Figure 9 shows a comparison of hysteresis characteristics in single- and triple-lead-plug types for L6 (γ = 200%, 60 cycles). It can be seen from Figure 9 (a) that the change of $Q_d$ in the triple-plug type was smaller than that in the single-plug type. This is considered to relate to the temperature of the specimen. As shown in Figure 9 (b), the temperatures of the triple-plug type were lower than those for the single-plug type (the temperature at measuring point P1 at 60 cycles was 107°C for the single-plug type and 47°C for the triple-plug type), and the temperature uptrend was also more gradual overall. In both cases, the temperature of the rubber (RC1) was lower than that of the lead (P1). In the LRB, it is considered that the lead absorbed seismic energy and therefore had a higher temperature than other parts of the specimen. Comparison of the triple-lead-plug type with the single-lead-plug type shows that the total volume of lead (which affects the calorific value) is the same, but the lead surface area (which affects heat dissipation) is larger in the former. This explains why the temperature of the triple-plug type was lower.

Figure 10 shows the relationships between horizontal force Q and horizontal displacement D for loading case L8. It can be seen that the shapes of the hysteresis curves are stable. The area enclosed by

the curve of the triple-lead-plug type is larger than that of single-plug type. The hysteresis curve of the former also shows a linear characteristic in the range of horizontal displacement up to about 200 mm and a hardening characteristic when this level is exceeded. The arrangement of three lead plugs is considered to have affected the stiffness of the laminated rubber bearing.

Although the horizontal restoration characteristic was greatly reduced by repeated deformation, it returned almost to its original state after the specimen temperature fell to the standard level of 25°C.

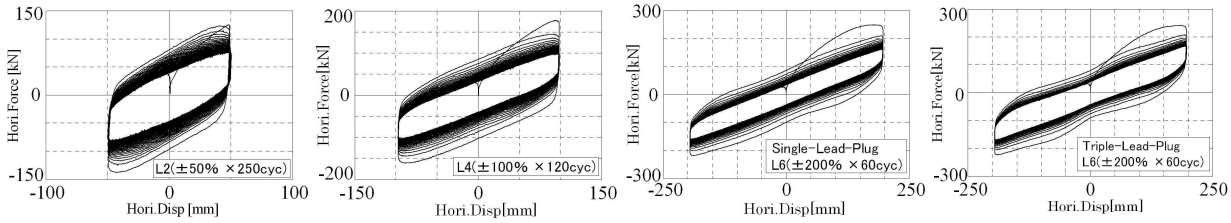


(a) L4 (γ = 50%) Single-lead-plug type

(b) L5 (γ = 100%) Single-lead-plug type

(c) L6 (γ = 200%) Single-lead-plug type

(d) L6 (γ = 200%) Triple-lead-plug type

**Figure 7.** Relationship between horizontal force Q and horizontal displacement D (LRB)

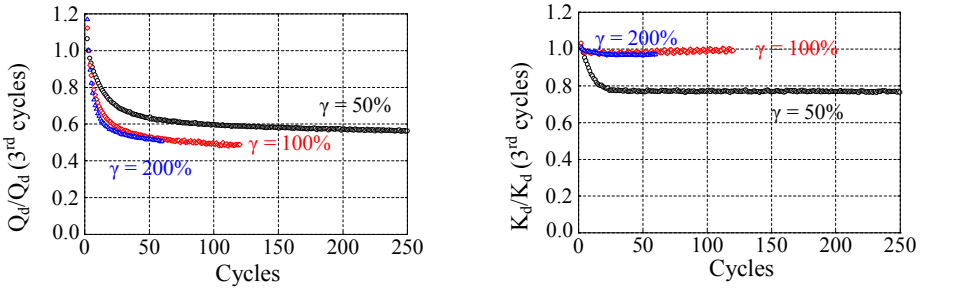


(a)Changes in yielding load $Q_d$

(b) Changes in stiffness $K_d$ after yielding

**Figure 8.** Changes in $Q_d$ and $K_d$ (Single-lead-plug type)

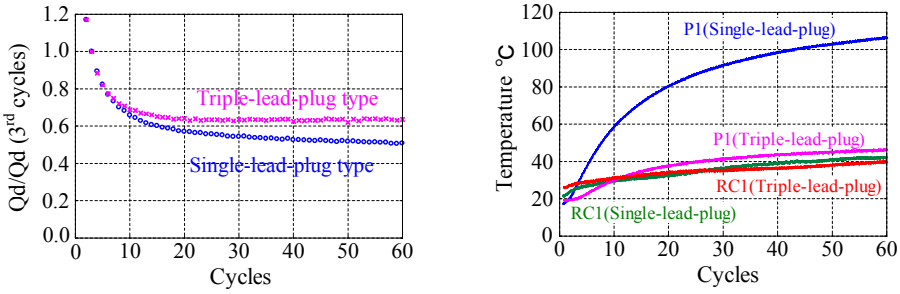


(a) Change of $Q_d$

(b) Temperature of specimen

**Figure 9.** Comparison in Single-lead-plug type and Triple-lead-plug type (L6)

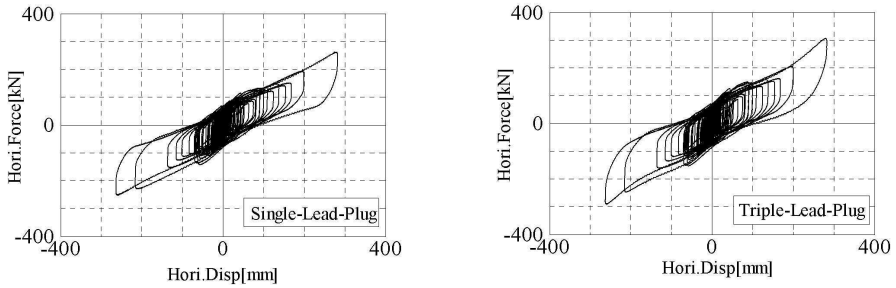


(a) Single-lead-plug type (L8)

(b) Triple-lead-plug type (L8)

**Figure 10.** Relationship between horizontal force Q and horizontal displacement D (LRB)

### 3.2 High Damping Rubber Bearing Experiments

*3.2.1. Method of determining HDRB hysteresis characteristics*

Changes in characteristics were determined based on the equivalent stiffness $K_{eq}$ and the equivalent damping factor $H_{eq}$. Based on Figure 11, $K_{eq}$ and $H_{eq}$ are represented by Eqn. 3.3 and 3.4. As the maximum displacement seen in the experiment did not cross the maximum load point, $K_{eq}$ can be taken as the secant stiffness of the virtual point connecting the positive and negative sides. $H_{eq}$ is calculated using $\Delta W$, $K_{eq}$ and $\delta_0$ (the average of the maximum displacement on the positive and negative sides). $K_{eq}$ and $H_{eq}$ are normalized with the third-cycle value.

$$K_{eq} = \frac{+Q-(-Q)}{+\delta_0-(-\delta_0)} \quad (3.3)$$

$$H_{eq} = \frac{\Delta W}{2\pi \times K_{eq} \times \delta_0^2} \quad (3.4)$$

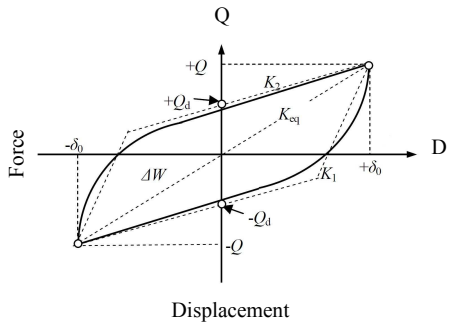


**Figure 11.** Definitions of $K_{eq}$, $H_{eq}$ and $\Delta W$

*3.2.2. Experiment results*

Figure 12 shows the relationships between horizontal force Q and horizontal displacement D, and Figure 13 shows temperatures measured during and after the experiment. In Figure 5, the measurement points are represented by ●.

From Figure 12, it can be seen that the area enclosed by the curve and the maximum load decreased as the number of repetitions increased for all cases.

For specimen #1H, the cumulative deformation was the same but the shear strain amplitude was different. Figure 13 (a) shows that even at the same level of cumulative deformation, larger amplitudes corresponded to greater temperature rises. The maximum temperature was 48°C for H1 ($\gamma$ = 50%, 1,000 cycles) and 90°C for H3 ($\gamma$ = 200%, 250 cycles).

The hysteresis curve for the initial temperature of 0°C shown in Figure 12 (d) is larger than that for 30°C shown in Figure 12 (e). That is, the specimen with an initial temperature of 0°C absorbed more energy overall than that at 30°C. However, the temperatures when the experiment ended (at about 1,000 seconds) were almost equal regardless of the initial level (Figure 13 (b)).

Comparison of gradual-increase loading with gradual-decrease loading indicates that the hysteresis characteristic and the rate of temperature rise differed, while the amounts of cumulative deformation were the same (Figures 12 (f), 12 (g) and 13 (c)). In particular, the difference in the hysteresis at $\gamma$ = 250% is significant, and the area enclosed by the curve for gradual-decrease loading is considerably reduced. From the above results, it is clear that changes in the horizontal characteristics of HDRB under multi-cycle loading are affected by the loading history.

The cumulative deformation of the earthquake response wave (H8) was about 14 m. This and the temperature rise of the specimen were both smaller than those seen in the sine wave experiment.

Figure 14 shows the relationship between the specimen temperature and the cumulative energy absorbed per unit volume of rubber (E/V). The temperature rose in proportion to the amount of energy absorbed.

Figure 15 shows changes in $K_{eq}$ and $H_{eq}$. $K_{eq}$ fell rapidly with larger amplitudes and lower initial specimen temperatures. The lower limits of the declines in $K_{eq}$ and $H_{eq}$ are considered to be about 0.6 times the value of the third cycle, respectively.

The horizontal restoration characteristics were significantly reduced by the repetition of horizontal deformation and lower initial temperature, but had returned almost to their original state a day after the experiments. The test results indicated that changes in characteristics stemming from multi-cyclic loading can be evaluated from changes in specimen temperature caused by the energy absorbed.

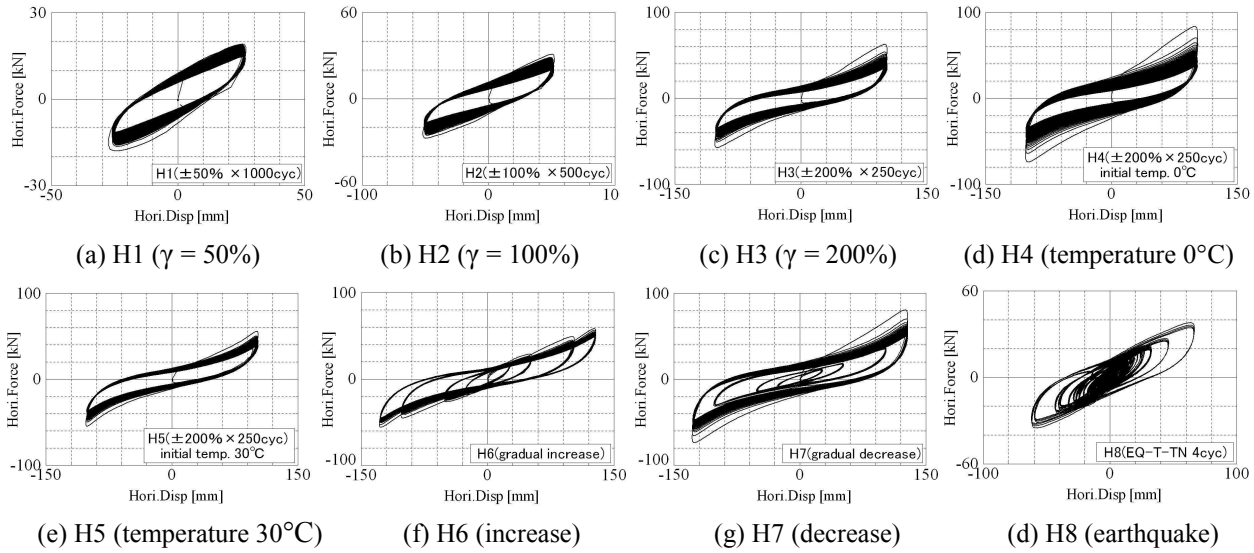


(a) H1 (γ = 50%) (b) H2 (γ = 100%) (c) H3 (γ = 200%) (d) H4 (temperature 0°C)

(e) H5 (temperature 30°C) (f) H6 (increase) (g) H7 (decrease) (d) H8 (earthquake)

**Figure 12.** Relationship between horizontal force Q and horizontal displacement D (HDRB)

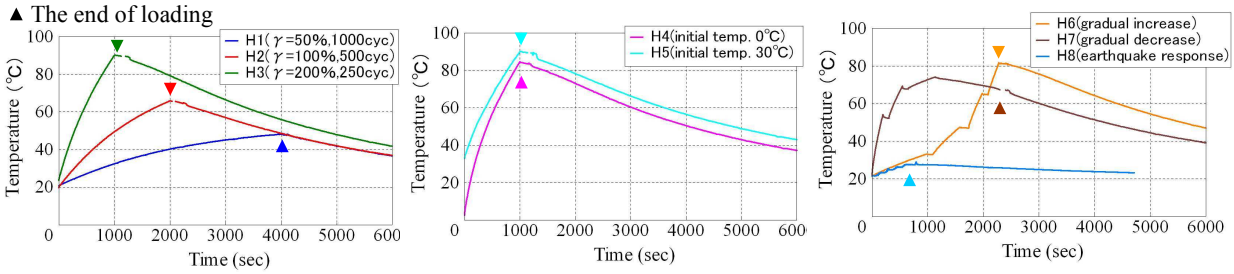


(a) H1, H2 and H3 (b) H4 and H5 (c) H6, H7 and H8

**Figure 13.** Specimen temperature

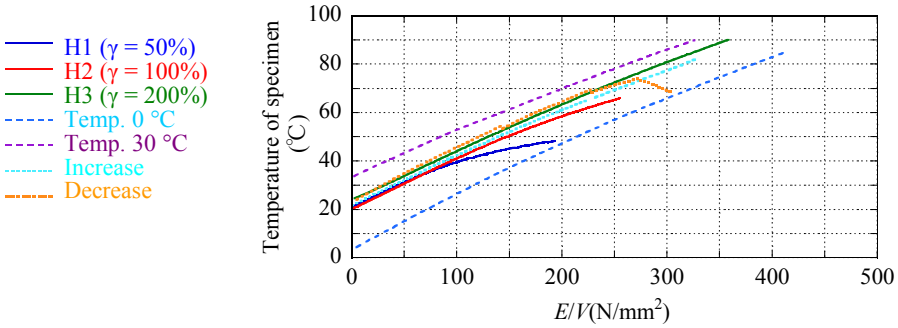


**Figure 14.** Relationship between cumulative energy absorbed and specimen temperatures

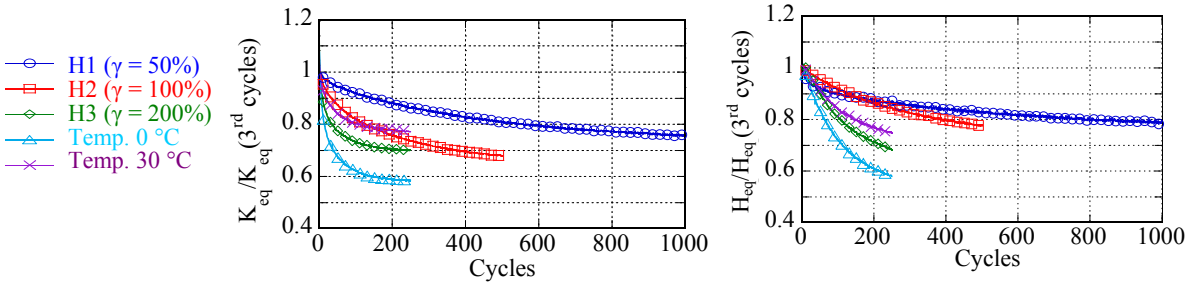


(a) Changes in equivalent stiffness $K_{eq}$ (b) Changes in equivalent damping factor $H_{eq}$

**Figure 15.** Changes in $K_{eq}$ and $H_{eq}$

## 4. CONCLUSION

To verify the performance of laminated rubber bearings against long-period ground motion, multi-cyclic loading tests of lead rubber bearings (LRBs) and high damping rubber bearings (HDRBs) using scaled rubber bearing specimens were conducted.

The LRB experiments clarified that increased lead plug temperatures led to reduced yield strength and damping performance. Even with identical levels of cumulative deformation, the yield strength fell as the amplitude increased. The rise in temperature was small in the multiple-lead-plug specimen (compared with single-lead plug type), which also exhibited a lower decrease in yielding load. As a result, the hysteresis curve of the multiple-lead-plug type became larger, and the plugs were also able to absorb more energy than that in the single-lead-plug type. Analytical verification of these phenomena such as heat-mechanics interaction analysis is a possible area for future study.

The hysteresis curves from the long-period ground motion test and the ultimate characteristic test showed a high level of mutual correspondence. That is, they were stabilized with a number of repetitions representing long-period ground motion, and the hysteresis characteristics did not change with numbers of repetitions exceeding this level.

In the HDRB experiments, the maximum load and the hysteresis loop area decreased and the specimen temperatures rose as the number of cycles increased. The degradation of hysteresis restoration characteristics in the horizontal direction and the temperature rise were more conspicuous with greater loading amplitudes, even though cumulative deformation was the same. The specimen with an initial temperature of 0°C absorbed more energy overall than that at 30°C. The specimen temperature rose in proportion to the amount of energy absorbed. The test results indicated that changes in characteristics stemming from multi-cyclic loading can be evaluated from specimen temperature changes caused by the energy absorbed.

Both in LRB and HDRB, the degradation of horizontal restoration characteristics was more conspicuous with greater shear strain amplitudes, even though cumulative deformation was the same. This means that the horizontal restoration characteristic decreases when the strain rate of loading increases. The horizontal characteristics of each specimen after the series of experiments were almost unchanged, and no apparent damage was observed. This indicates that LRB and HDRB have the large capacity to stably absorb the seismic energy produced by long-period ground motion.

Establishment of a method to evaluate mechanical property changes caused by repetitive motion for structural design will be a key consideration in future research.

**ACKNOWLEDGEMENT**

This paper describes a part of productions of the promotion project for building-standards maintenance "27-3 Examination about the safety verification method of the seismically isolated buildings against long-period ground motions" conducted by the Ministry of Land, Infrastructure and Transport in the Heisei 22 fiscal year. Gratitude is respectfully expressed to the main committee (chairperson: Professor Haruyuki Kitamura of Tokyo University of Science), WG for testing of devices (chief examiner: Professor Mineo Takayama of Fukuoka University), WG for evaluation of response of buildings (chief examiner: Professor Takeshi Furuhashi of Nihon University) and all the persons concerned.

**REFERENCES**

1) Takaoka, E., Takenaka, Y., Kondo, A., Hikita, M. and Kitamura, H. (2008). Heat-Mechanics Interaction behaviour of laminated rubber bearings under large and cyclic lateral deformation. *The 14th World conference on earthquake engineering,* No.1241

2) Kitamura, H., Hayakawa, S., Takenaka, Y., Takaoka, E. and Murota, N. (2010). Evaluation of the influence of heat-mechanics interaction behaviour in high-damping rubber bearings on seismic response of base-isolated buildings. *Journal of Structural and Construction Engineering*, Vol. 75, No.655, 1635-1644

3) Architectural Institute of Japan. (2007). Structural response and performance for long period seismic ground motions. *Architectural Institute of Japan*

4) Shimizu Corporation and The Japan Society of Seismic Isolation, et al. (2010). 12 Examination to contribute to maintenance of standard law of base-isolated buildings. *Productions of the promotion project for building-standards maintenance by Ministry of Land, Infrastructure and Transport*, FY2009 Report.